Model for transmission of ultrastrong laser pulses through thin foil targets

Wei Yu,[1,2] Z. M. Sheng,[3,*] M. Y. Yu,[1] J. Zhang,[4] Z. M. Jiang,[5] and Z. Xu[5]
[1]*Institut für Theoretische Physik I, Ruhr-Universität Bochum, D-44780 Bochum, Germany*
[2]*Shanghai Institute of Optics and Fine Mechanics, Shanghai 201800, People's Republic of China*
[3]*Max-Planck-Institut für Quantenoptik, D-85748 Garching, Germany*
[4]*Institute of Physics, Beijing 100080, People's Republic of China*
[5]*INRS–Energie et Matériaux, 1650 Boulevard Lionel Boulet, Case Postale 1020, Varennes, Québec, Canada J3X IS2*
(Received 24 September 1998)

A model for the penetration of ultrahigh-intensity ultrashort-pulse lasers through a highly overdense foil target is proposed. The model involves only electron motion. It is shown that the ponderomotive force of the light waves can push the electrons towards the back surface of the foil, such that the effective thickness of the latter is reduced to the order of the skin depth, thus allowing wave penetration. The results agree well with that from a particle-in-cell simulation. [S1063-651X(99)13803-0]

PACS number(s): 52.35.Ra, 52.35.Mw, 52.35.Qz

I. INTRODUCTION

The interaction between ultrahigh-intense ultrashort-pulse lasers and overdense plasmas with densities many orders of magnitude higher than that of critical is a topic of recent interest since it leads to many novel applications. The latter include fast ignition in inertial confinement fusion [1,2], absorption and propagation of femtosecond laser pulses in solid density plasmas [3–9], coherent soft x-ray sources from the high harmonics generated by interaction [10], etc. In most experiments using fs laser pulses at focused intensities of the order 10^{18} W/cm^2 the appearance of preformed plasmas is inevitable, because the intensity of the laser-pulse pedestal produced by the amplified spontaneous emission in the laser train or residual dispersion of the recompression in the chirped pulse amplification can be higher than the threshold intensity for plasma formation [11–13] since the pulse pedestal-to-peak contrast ratio of existing solid-state laser technology is only of the order 10^6 [14]. It is therefore important to avoid the pulse pedestal by appropriately reshaping the pulse, such that a clean interaction of the laser pulse with a solid density plasma can be realized.

Recently, it has been shown [11,15] that near total transmission of a 30 fs, 3×10^{18} W/cm^2 laser pulse through a thin (0.1 μm) plastic foil target is possible. It was also found that at 5×10^{16} W/cm^2 the transmittivity in the same system was reduced to the background level of 1%. The strong intensity dependence of the foil transparency was attributed to an unknown mechanism, since it seems that all the known ones [16–21] such as anomalous skin effect, hole boring, and classical self-induced transparency, can be ruled out [15]. The high transmittivity in such thin plastic foils has the obvious important potential application of reshaping laser pulses [15].

To explore the physical mechanism of the anomalously high transmittivity seen in the recent experiments we present here a simple self-consistent model for the transmission of an intense short-pulse laser through a thin-foil target. The model is based on the idea that the ultra-intense light pressure of an ultrashort light pulse compresses the electrons in the thin target into a much thinner layer before significant ion motion sets in, such that the effective target width as seen by the laser becomes of the order of or less than the skin depth. For analytical simplicity, the normal incidence of a circularly polarized laser pulse onto a highly overdense thin plasma layer is considered. It is found that the transmittivity can increase rapidly with the laser strength parameter when the latter is above 3. For circularly polarized light the transmittivity is found to be about 42% for an ion density 50 times critical, laser strength parameter 3, and foil thickness 0.1 times the wavelength. This result agrees well with that from a particle-in-cell (PIC) simulation. Although because of physical as well as mathematical complexity we have not presented an analytical theory for linearly polarized light, simulation shows that near 100% transmission occurs for the same parameters as that of the circularly polarization case.

II. FORMULATION

For very high power and short-pulse laser interaction with thin foils, the electron quiver motion dominates over that of thermal, so that electron-ion collisions and electron heating effects can be neglected [22]. For the same reason, the plasma ions do not react significantly during the time of the interaction, so that one can neglect the hydrodynamic motion of the plasma and assume a steplike profile for the immobile ions: $n_i=\text{const}$ for $0\leqslant z\leqslant z_d$, and $n_i=0$ elsewhere. In reality, for present-day lasers the original ion profile could not be maintained for the entire interaction process and the ions can also be compressed. However, since according to our proposal the laser-light penetration is mainly due to the reduction of the thickness of the electron layer, the change of the ion profile does not directly affect the results. These assumptions are verified *a posteriori* by numerical simulations.

For the electron velocity $\mathbf{w}$ we set $\mathbf{w}=\mathbf{u}+\mathbf{v}$, where $\mathbf{u}$ and $\mathbf{v}$ are the transverse and longitudinal components satisfying $\nabla\cdot\mathbf{u}=0$ and $\nabla\times\mathbf{v}=\mathbf{0}$, respectively. From the Maxwell equations we have

*Present address: Institute of Laser Engineering, Osaka University, 2-6 Yamada-oka, Suita, Osaka 565, Japan.

$$c^2\nabla^2\mathbf{A}-\partial_t^2\mathbf{A}=4\pi cen\mathbf{u}, \tag{1}$$

$$4\pi en\mathbf{v}+\partial_t\nabla\phi=\mathbf{0}, \tag{2}$$

$$\nabla^2\phi=4\pi e(n-Zn_i), \tag{3}$$

where $\mathbf{A}$ is the vector potential satisfying the Coulomb gauge $\nabla\cdot\mathbf{A}=0$, ϕ is the scalar potential describing the electrostatic field of the charge separation, n and n_i are the electron and ion densities, and Z is the ion charge number.

If the laser spot size is much larger than the target thickness x_d, we can use the planar geometry [18] and write $\mathbf{A}=A(z,t)(\hat{\mathbf{x}}+\hat{\mathbf{y}})$, $\phi=\phi(z,t)$, $\mathbf{u}=u(z,t)(\hat{\mathbf{x}}+\hat{\mathbf{y}})$, and $\mathbf{v}=v(z,t)\hat{\mathbf{z}}$. In view of the very low collision rate in the high-intensity wave field, absorption of laser energy by the target electrons will be neglected. Substituting the Lagrangian of a relativistic electron into the Euler-Lagrange equation we get

$$d_t(m\gamma\mathbf{u}-e\mathbf{A}/c)=\mathbf{0}, \tag{4}$$

$$d_t(m\gamma v)+mc^2\partial_z\gamma-e\partial_z\phi=0 \tag{5}$$

for the transverse and longitudinal electron motion. Thus, we have $\mathbf{u}=e\mathbf{A}/mc\gamma$.

For circular polarization the ponderomotive force, the relativistic factor, as well as the charge separation field are time independent [23]. From Eq. (2) we have $v=0$ and the important relation $\gamma=(1-\mathbf{u}\cdot\mathbf{u}/c^2)^{-1/2}=(1+|a|^2)^{1/2}$, where $a=eA/mc^2$ is the electron quiver velocity normalized by c. Equations (3) and (5) can be rewritten as

$$\partial_\xi^2\psi=N-N_i, \tag{6}$$

$$\partial_\xi\gamma=\partial_\xi\psi, \tag{7}$$

where $\xi=\omega z/c$, $\psi=e\phi/mc^2$, $N=n/n_c$, $N_i=Zn_i/n_c$, and $n_c=m\omega^2/4\pi e^2$ is the critical density. On the other hand, Eq. (1) yields

$$a^{-1}\partial_\xi^2 a+1-N\gamma^{-1}=0 \tag{8}$$

for the normalized vector potential. In the following we shall solve the governing equations in each region. By matching the solutions at the boundaries using appropriate particle and electromagnetic field continuity conditions, the integration constants are determined in a self-consistent manner.

III. SOLUTIONS

Equations (6)–(8) were first studied by Lai [23]. Physically, under very large laser pressure the target electrons near the surface are rapidly pushed inward, leaving behind a positively charged layer in $0\leqslant\xi<\xi_b$ [23,24], where the immobile ions have no effect on the electromagnetic fields. The affected electrons are compressed into a region $\xi_b\leqslant\xi\leqslant\xi_d$. In this region the electron density, the charge separation field, the value of ξ_b, as well as the laser fields can be determined in a self-consistent manner.

We set $a=|a|\exp(i\theta)$ and obtain from Eqs. (6)–(8) two constants of motion [23]:

$$\mathcal{M}=(\gamma^2-1)\partial_\xi\theta, \tag{9}$$

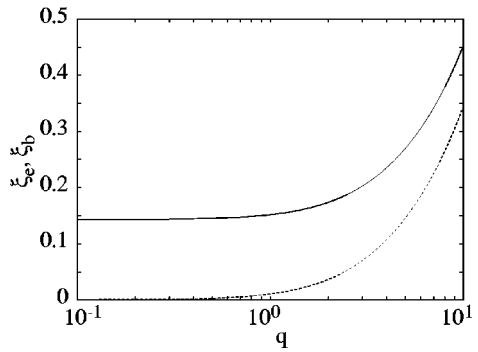

FIG. 1. The normalized depths ξ_b of the positively charged layer and ξ_e of laser penetration *vs* the laser strength q.

$$\mathcal{W}=[\mathcal{M}^2+(\partial_\xi\gamma)^2]/(\gamma^2-1)-\gamma(2N_i-\gamma), \tag{10}$$

where $\mathcal{M}$ is proportional to the electromagnetic energy flux flowing across the target. It may be written as $\mathcal{M}=Tq^2$, where $q=|a(\xi=0)|=e|E_i|/m\omega c=0.85\times10^{-9}\lambda\sqrt{I}$ is the laser strength parameter, $T=I_t/I=|E(d)|^2/|E(0)|^2$ is the transmittivity, λ is the laser wavelength in μm, and $I=(c/8\pi)|E_i|^2$ and $I_t=(c/8\pi)|E_t|^2$ are the intensities (in W/cm^2) of the incident and transmitted laser lights. Furthermore, $(\partial_\xi\theta)^2$ may be identified as the plasma dielectric constant [23].

The amplitudes of the electric and magnetic fields of the laser light can be expressed as

$$|E|^2=\gamma^2-1, \tag{11}$$

$$|B|^2=\gamma^2\mathcal{W}+\gamma^3(2N_i-\gamma)-M^2, \tag{12}$$

where we have noted that $|E|^2=|a|^2$ and $|B|^2=(\partial_\xi|a|)^2+|a|^2(\partial_\xi\theta)^2$. The electron density and charge separation field are given by

$$N=\gamma(3N_i\gamma-2\gamma^2+1+\mathcal{W}), \tag{13}$$

$$E_0=[(\mathcal{W}+2N_i\gamma-\gamma^2)(\gamma^2-1)-\mathcal{M}^2]^{1/2}, \tag{14}$$

where $E_0=-\partial_\xi\gamma$.

The field quantities in the different regions are related through the usual electromagnetic field boundary conditions [25] at $\xi=\xi_b$ and $\xi=\xi_d$. Accordingly, the continuity of the laser fields at $\xi=\xi_b$ yields $|E_b|^2/q^2=4/|1+\chi|^2$ with $\chi=B_b/E_b$, or

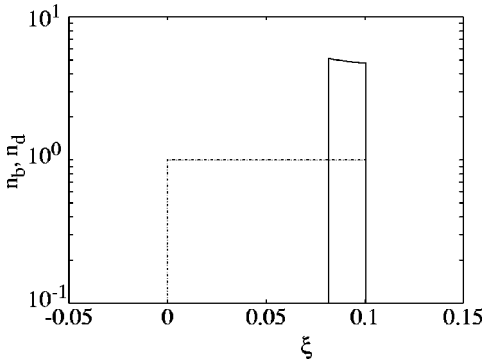

FIG. 2. The normalized electron (solid curve) and ion (dashed curve) density profiles for $N_i=50$, $q=3$, and $\xi_d=0.1$.

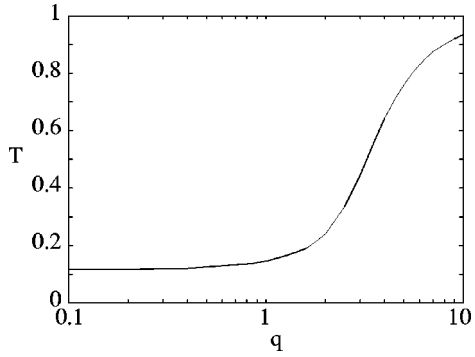

FIG. 3. The transmittivity T *vs* the laser strength q for $N_i=50$ and $\xi_d=0.1$.

$$4q^2(\Gamma_b^2-1)=(\mathcal{M}+\Gamma_b^2-1)^2+\Gamma_b^2(\partial_\xi\gamma)_b^2, \qquad (15)$$

where Γ_b is the value of γ at $\xi=\xi_b$. On the back side of the target foil, the transmitted radiation propagates into a vacuum with $|E|^2=|B|^2=\mathcal{M}$, and the continuity of the laser fields at $\xi=\xi_d$ leads to $\mathcal{W}=2\mathcal{M}+1-2N_i(\mathcal{M}+1)^{1/2}$. Finally, charge conservation requires $N_i\xi_b=\int_{\xi_b}^{\xi_d}(N-N_i)d\xi$, which yields

$$\xi_b=[(\mathcal{W}+2N_i\Gamma_b-\Gamma_b^2)(\Gamma_b^2-1)-\mathcal{M}^2]^{1/2}/N_i \qquad (16)$$

for the thickness of the positive layer. Thus, the effective target thickness becomes $\xi_d-\xi_b$.

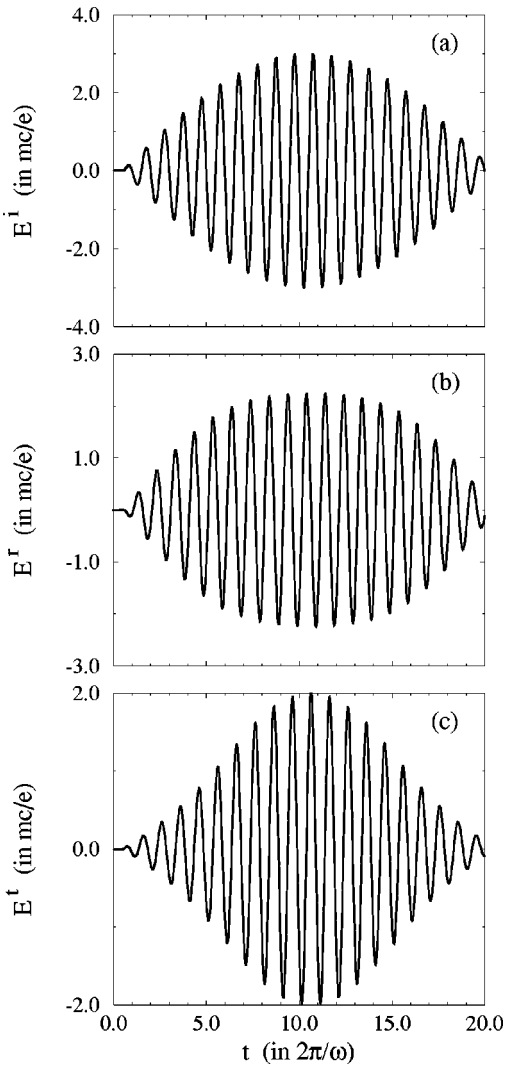

FIG. 4. Simulation of the interaction of a circularly polarized sine pulse of $q=3$ and a plasma of fixed ion profile with $N_i=50$ and $\xi_d=0.1$: the (a) incident (E^i), (b) reflected (E^r), and (c) transmitted (E^t) profiles of the normalized laser electric field.

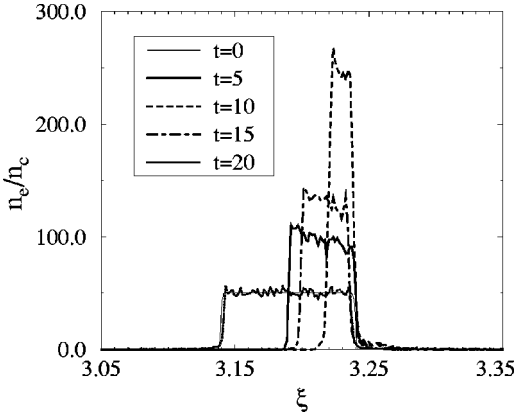

FIG. 5. Same simulation as for Fig. 4. Evolution of the normalized electron density during the interaction. The square profile represents the ion or initial electron density.

Physically, the compression of the electrons arises from the relativistic ponderomotive force. The effective skin depth of the laser light is given by $\xi_s\sim\sqrt{\gamma/N}$. It is of interest to note that if there were no compression, we have $N=N_i$ and the skin depth would actually increase by a factor $\sqrt{N/N_i}$. But in this case the laser sees the original foil thickness of ξ_d.

IV. RESULTS

We first consider the case of total reflection, for which $\mathcal{M}=0$ and the laser radiation evanescences inside the target with $\gamma\to1$ and $\gamma_\xi\to0$. Figure 1 shows the dependence of the depth ξ_b of the positively charged layer and the depth ξ_e of laser penetration on the laser strength q. The penetration depth ξ_e is defined to be the distance at which the radiation is damped to $1/e$ of its value at the target surface. As expected, for $q\ll1$ the laser penetration into the target is of the order of the skin depth, which is determined only by the target density N_i. It increases slowly with q. At higher laser strengths $(q>1)$, however, the penetration depth becomes strongly intensity dependent. The increase in the laser penetration is associated with the increase of the size of the positively charged layer resulting from the strong compression of the electrons towards the backside of the target.

One may expect that for plasma layers of effective thickness smaller than the penetration depth, a part of the laser energy will be transmitted. Figure 2 shows the electron (solid curve) and ion (dashed curve) density profiles of an interaction with $N_i=50$, $q=3$, and $\xi_d=0.1$. One finds $T=0.42$, or about half of the incident radiation is transmitted. Figure 3 shows the dependence of the transmittivity T on the laser strength q for a foil target with $N_i=50$ and $\xi_d=0.1$. For lower laser intensities $(q<1)$, there is an almost strength-

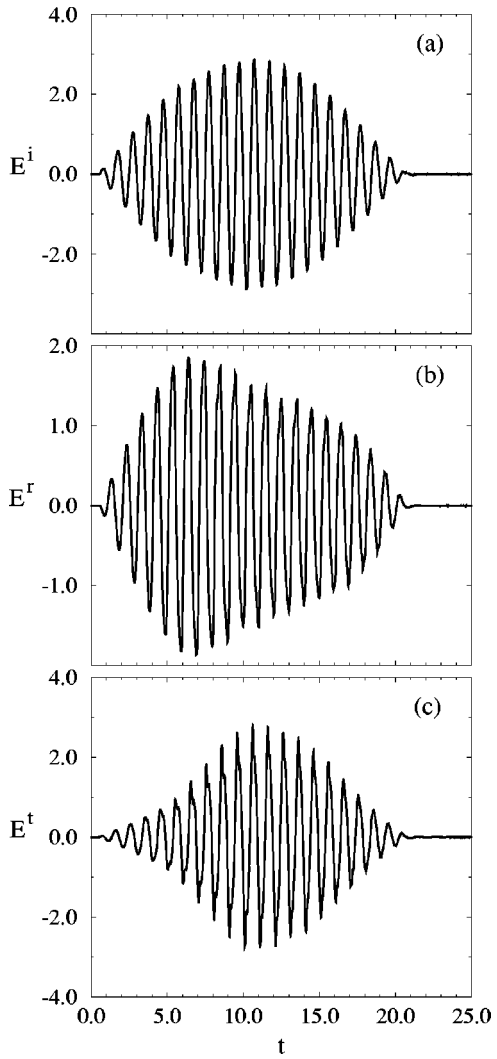

FIG. 6. Simulation of the interaction of a *linearly* polarized sine pulse of $q=3$ and a plasma with $N_i=50$ and $\xi_d=0.1$: the (a) incident (E^i), (b) reflected (E^r), and (c) transmitted (E^t) profiles of the laser electric field.

independent transmittivity of about 10%. For higher intensities ($q>1$), the transmittivity rapidly increases with q and the target can become very transparent. It is evident that this effect has the potential application for reshaping laser pulses: the less intense pedestal will be reflected and the peak of the main pulse will be transmitted.

V. PIC SIMULATIONS

To verify our assumptions and results, we have performed numerical simulations using the LPIC++ PIC code [26]. A sine pulse of $q=3$ is incident upon a plasma with ions of fixed square density profile $N_i=50$ and $\xi_d=0.1$. The code was run with and without the ion dynamics. It was found that in general the ion are also compressed during the laser-plasma interaction, but the main results on laser penetration/reflection are not much affected. This is expected since hf electromagnetic waves and their skin depth are not directly affected by the heavy ions.

The incident, reflected, and transmitted profiles of the laser electric field are shown in Figs. 4(a), 4(b), and 4(c), respectively. We see that the high-intensity part of the laser pulse has higher transmittivity than the less intense parts. As a result, the transmitted pulse is reshaped. At maximum amplitude the transmittivity for the case considered is up to 44%, which is in good agreement with the theoretical prediction (see Fig. 3). Note that in the present example (q is relatively low for the circularly polarized light) the reflected pulse has a sharper rising front and higher amplitude than that of the transmitted one. The situation is reversed for higher q values. Thus, for pulse reshaping it is necessary to optimize the thickness of the foil, so that initially it should be larger than the skin depth such that the low-energy part of the pulse cannot tunnel through.

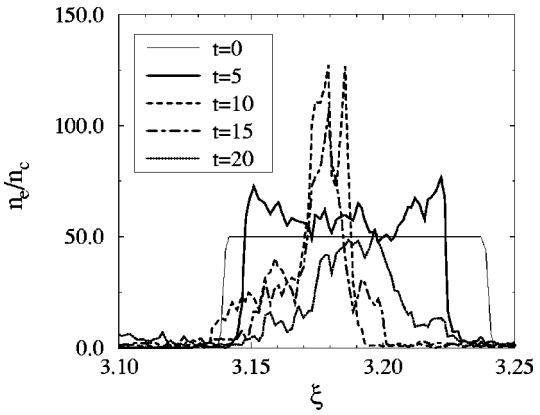

FIG. 7. Same simulation as for Fig. 6. Evolution of the electron density during the interaction.

In Fig. 5 the evolution of the electron density during the passage of the laser pulse is shown. The square profile represents the electron density at $t=0$ (or the ion density). As the pulse enters the plasma with increasing strength, the electrons are pushed further and further towards the back of the target, reaching nearly fivefold (electron) density compression at the peak laser amplitude. After that, the laser field strength diminishes and the electrostatic field of charge separation draws back the electrons, until the target nearly restores to its original state after the pulse is over.

VI. DISCUSSION

In this paper, we have for the sake of simplicity (in that analytical calculations are possible) considered fixed ion profiles and circularly polarized lasers. In the real situation, the ion density profile cannot remain constant during the entire interaction period. There can therefore exist high density-gradient transition regions between the ones considered here. However, since electron heating is weak because of negligible collisions, and we have used exact boundary conditions for the electromagnetic wave fields (that is, the gradient layers are approximated as having zero thickness without losing the overall physical characteristics [25]), our conclusion on laser transmission is not significantly affected by the immobile-ion assumption, as is also verified by numerical simulations.

For linearly polarized lasers, new physical processes can enter. Electron oscillations may be driven by the longitudinal component of the laser electric field and/or the oscillating ponderomotive field at twice the laser frequency [27]. In this

case, the electrons can be pulled out of the target into the front vacuum region and sent back again by the oscillations. But not all electrons will return in each cycle, and the stray ones will form an electron cloud in front of the target [28]. Clearly, the same process can occur at the backside of the target foil if there is transmission of the laser light. The underdense clouds can lead to additional phenomena such as resonant acceleration of the electrons [28], backside ponderomotive compression of the electrons, etc., and the problem is considerably more involved. On the other hand, the appearance of the clouds, approximately 0.5λ in size, leads to a strong reduction of the compressed electron number density inside the target. Thus the transmittivity can be expected to increase significantly over the case of circular polarization.

To verify the above point, we carried out a PIC simulation for linearly polarized light with the same parameters as that for the circular polarization case. The results are presented in Figs. 6 and 7. We see that the transmittivity is near 100%. Such a high transmittivity was observed experimentally by Giulietti *et al.* [15]. Furthermore, the reflected and transmitted light pulses are strongly modulated and the target electrons are compressed to near the center of the layer, indicating simultaneous front- and back-side ponderomotive compression. We also note that the compressed electron density is much reduced compared with the circular polarization case, since many electrons are ejected into the front and back vacuum regions. An analytical theory for the interaction of a linearized polarized laser with thin-foil targets is still under development.

ACKNOWLEDGMENTS

This work was partially supported by the Sonderforschungsbereich 191 Niedertemperatur Plasmen. One of the authors (W.Y.) would like to thank the K. C. Wong Education Foundation, the Deutscher Akademischer Austauschdienst, and the National High-Technology Program of China (Contract Nos. 863-416-1 and 863-416-3) for financial support. We thank R. Lichter, R. Pfund, and J. Meyer-ter-Vehn for the use of their LPIC++ PIC code.

[1] D. Strickland and G. Mourou, Opt. Commun. **56**, 219 (1985).
[2] M. Tabak *et al.*, Phys. Plasmas **1**, 1626 (1994).
[3] F. Brunel, Phys. Rev. Lett. **59**, 52 (1987).
[4] J.C. Kieffer *et al.*, Phys. Rev. Lett. **62**, 760 (1989).
[5] P. Gibbon and A. Bell, Phys. Rev. Lett. **68**, 1535 (1992).
[6] S.C. Wilks *et al.*, Phys. Rev. Lett. **69**, 1383 (1992).
[7] U. Teubner *et al.*, Phys. Rev. Lett. **70**, 794 (1993).
[8] A. Pukhov and J. Meyer-ter-Vehn, Phys. Rev. Lett. **79**, 2686 (1997).
[9] J. Fuchs *et al.*, Phys. Rev. Lett. **80**, 2326 (1998).
[10] P.A. Norreys *et al.*, Phys. Rev. Lett. **76**, 1832 (1996).
[11] M.P. Kalashnikov *et al.*, Phys. Rev. Lett. **73**, 260 (1994).
[12] L.A. Gizzi *et al.*, Phys. Rev. Lett. **76**, 2278 (1996).
[13] Y. Zhang *et al.*, Opt. Commun. **126**, 85 (1996).
[14] C. Danson *et al.*, Opt. Commun. **103**, 392 (1993).
[15] D. Giulietti *et al.*, Phys. Rev. Lett. **79**, 3194 (1997).
[16] W. Rosmus and V. Tikhonchuk, Phys. Rev. A **42**, 7401 (1990).
[17] S.C. Wilks *et al.*, Phys. Rev. Lett. **69**, 1383 (1992).
[18] S. Kato *et al.*, Phys. Fluids B **5**, 564 (1993).
[19] G. Malka and J.L. Miquel, Phys. Rev. Lett. **77**, 75 (1996).
[20] R. Kodama *et al.*, Phys. Rev. Lett. **77**, 4906 (1996).
[21] E. Lefebvre and G. Bonnaud, Phys. Rev. Lett. **74**, 2002 (1997).
[22] C.D. Decker, W.B. Mori, J.M. Dawson, and T. Katsouleas, Phys. Plasmas **1**, 4043 (1994).
[23] C.S. Lai, Phys. Rev. Lett. **36**, 966 (1976).
[24] R.N. Sudan, Phys. Rev. Lett. **70**, 3075 (1993).
[25] J.D. Jackson, *Classical Electrodynamics* (Wiley, New York, 1975).
[26] R. Lichter, R. E. W. Pfund, and J. Meyer-ter-Vehn, *LPIC++ A Parallel One-dimensional Relativistic Electromagnetic Particle-in-cell Code for Simulating Laser-plasma-Interaction*, Report MPQ225 (Max-Planck-Institut für Quantenoptik, Garching, 1997).
[27] W. Yu, M.Y. Yu, J. Zhang, and Z. Xu, Phys. Rev. E **57**, R2531 (1998).
[28] W. Yu, M.Y. Yu, Z.M. Sheng, and J. Zhang, Phys. Rev. E **58**, 2456 (1998).